The Journal of Neuroscience

http://jneurosci.msubmit.net

JN-RM-3621-15R1

Effective Connectivity from Early Visual Cortex to Posterior Occipito-temporal Face Areas Predicts Developmental Prosopagnosia

Michael Lohse, University of Oxford
Brad Duchaine, Dartmouth College
Lucia Garrido, Brunel University London
Jon Driver,
Raymond Dolan, Wellcome Trust Centre for Neuroimaging, UCL
Nicholas Furl, Royal Holloway, University of London

Commercial Interest:

Effective Connectivity from Early Visual Cortex to Posterior Occipito-temporal Face Areas Supports Face Selectivity and Predicts Developmental Prosopagnosia

Running Title: Effective connectivity and face perception ability

Michael Lohse[1,2], Bradley C. Duchaine[3], Lucia Garrido[4], Jon Driver[5,6], Raymond J. Dolan[5], Nicholas Furl[1,7]

[1] Medical Research Council, Cognition and Brain Sciences Unit, 15 Chaucer Road, Cambridge CB2 7EF, United Kingdom

[2] Department of Physiology, Anatomy, and Genetics, University of Oxford, Oxford OX1 3QX, United Kingdom

[3] Psychological and Brain Sciences, Dartmouth College, Hanover, NH 03755, USA

[4]Division of Psychology, Department of Life Sciences, Brunel University London, Uxbridge UB8 3PH, United Kingdom

[5] Wellcome Trust Centre for Neuroimaging, University College London WC1N 3BG, United Kingdom

[6] Institute of Cognitive Neuroscience, University College London, London WC1N 3AR, United Kingdom

[7] Department of Psychology, Royal Holloway, University of London, Egham Hill, Egham, Surrey, TW20 0EX, United Kingdom

Corresponding author:

Michael Lohse

Department of Physiology, Anatomy, and Genetics, University of Oxford

michael.lohse@sjc.ox.ac.uk

23 pages, 4 figures, 1 table

Abstract (238 words), Introduction (648), Discussion (1280 words)

We declare no conflict of interest

Acknowledgements

This work was supported by the Wellcome Trust (ML (105241/Z/14/Z), R. J. D., and J. D.). J.D. was a Royal Society Research Professor when the research was performed. The authors are grateful to their colleagues at the University College London, namely, Laura Germine and Raka Tavashmi for assistance with behavioral measurement and/or fMRI data collection, and John Stevens for clinical evaluation of the participants.

Abstract

Face processing is mediated by interactions between functional areas in the occipital and temporal lobe, and the fusiform face area (FFA) and anterior temporal lobe play key roles in the recognition of facial identity. Individuals with developmental prosopagnosia (DP), a lifelong face recognition impairment, have been shown to have structural and functional neuronal alterations in these areas. The present study investigated how face selectivity is generated in participants with normal face processing, and how functional abnormalities associated with DP, arise as a function of network connectivity. Using functional magnetic resonance imaging and dynamic causal modeling, we examined effective connectivity in normal participants by assessing network models that include early visual cortex (EVC) and face-selective areas and then investigated the integrity of this connectivity in participants with DP. Results showed that a feedforward architecture from EVC to the occipital face area, EVC to FFA, and EVC to posterior superior temporal sulcus (pSTS) best explained how face selectivity arises in both controls and participants with DP. In this architecture, the DP group showed reduced connection strengths on feedforward connections carrying face information from EVC to FFA and EVC to pSTS. These altered network dynamics in DP contribute to the diminished face selectivity in the posterior occipito-temporal areas affected in DP. These findings suggest a novel view on the relevance of feedforward projection from EVC to posterior occipito-temporal face areas in generating cortical face selectivity and differences in face recognition ability.

Significance statement

Areas of the human brain showing enhanced activation to faces compared to other objects or places have been extensively studied. However, the factors leading to this face selectively have remained mostly unknown. We show that effective connectivity from early visual cortex to posterior occipito-temporal face areas gives rise to face selectivity. Furthermore, people with developmental prosopagnosia, a lifelong face recognition impairment, have reduced face selectivity in the posterior

occipito-temporal face areas and left anterior temporal lobe. We show that this reduced face selectivity can be predicted by effective connectivity from early visual cortex to posterior occipito-temporal face areas. This study presents the first network-based account of how face selectivity arises in the human brain.

1. Introduction

During the last two decades, functionally-localized areas relevant for face processing in humans have been investigated. These face-selective areas show stronger blood oxygen level dependent (BOLD) responses to faces compared to other objects (Kanwisher et al., 1997). However, these areas do not function in isolation but rather as an integrated system (Moeller et al., 2008). A model of the functional integration of face-selective areas is required to understand the neural underpinnings of face processing. Most previous studies investigating connectivity in face-selective networks have focused on anatomical connections (Gomez et al., 2014; Thomas et al., 2008) or correlated BOLD responses between face-selective areas (functional connectivity) (George et al., 2001; Iidaka et al., 2001). A handful of studies have focused on the direction of information flow between face-selective areas (Fairhall and Ishai, 2007; Furl et al., 2013). A common limitation of these directional connectivity studies is that they do not isolate the flow of face-selective information from other information. Those few studies of the directional flow of face-selective information, used network models limited to relatively few face-selective regions (Furl et al., 2014; Nagy et al., 2012). Here, we investigate the directional flow of face-selective information using the most comprehensive face processing network investigated to date. We further compare the flow of face-selective information between controls and people with developmental prosopagnosia (DP), a lifelong face recognition impairment.

Previous theory can guide hypotheses about the factors generating face-selectivity. An influential proposal for the neural architecture for face processing separates face-selective areas into

a core system that carries out visual analysis and which consists of the occipital face area (OFA), fusiform face area (FFA), and posterior superior temporal sulcus (pSTS), and an extended system carrying out further, higher level processing (Haxby et al., 2000). Extended areas process information such as knowledge about the owner of a face in the anterior temporal lobe (ATL) and emotional information in the amygdala. Formal models testing how interactions between these areas give rise to face-selectivity have not been developed. Our first aim was to quantitatively compare plausible connectivity architectures, using dynamic causal modeling (DCM) (Friston et al., 2003).

Occipito-temporal contributions to face processing can be investigated by studying individuals with DP. People with DP have difficulty recognizing facial identity (Behrmann & Avidan, 2005; Duchaine & Nakayama, 2006) and sometimes have problems with other aspects of face processing as well (Duchaine et al., 2006; Nunn et al., 2001). Neural abnormalities in DPs have been reported. Berhmann et al. (2007) and Garrido and colleagues (2009) reported decreased grey matter in the fusiform gyrus, STS and ATL of participants with DP. Gomez et al. (2014) and Song et al. (2015) found altered white matter around FFA in DP. Furl and colleagues (2011) examined DP individuals and typical controls and showed that BOLD responses in bilateral FFA and ATL correlated with face recognition ability. Furthermore, Furl et al. (2011), Dinckelacker et al. (2011), and von Kriegstein et al. (2008) found participants with DP had reduced face selectivity in FFA. Avidan et al. (2014) found reduced activation in ATL, and reduced functional connectivity between the core system and ATL in DP. To better understand decreased face selectivity asscoiated with the DP population, our second aim was to contrast neural connectivity in participants with DP versus participants with normal face recognition.

To establish the network architecture of face processing, we estimated the directionality of informational flow, using DCM, when participants viewed faces. We further investigated the relevance of the state of this system for behavior by identifying how it is altered in DP. We found a network that best explains how face relevant information flows through a face-selective network where the presence or absence of faces modulates connectivity from early visual cortex (EVC) to

posterior occipito-temporal areas (OFA, FFA, and pSTS). Also, We further show that the strength of face-specific modulation in connections from EVC to FFA and pSTS is diminished in DP.

2.Method

2.1. Participants

We examined the same 15 DP and 15 control individuals from Garrido et al. (2009) who returned for the fMRI experiment reported in Furl et al. (2011). The participants with DP reported great difficulties with face recognition in daily life and were diagnosed using the Cambridge Face Memory Test (CFMT in its original form; Duchaine & Nakayama, 2006a) and the Famous Faces Test (FFT; Duchaine & Nakayama, 2005). Informed consent was obtained in accordance with procedures approved by The Joint Ethics Committee of The National Hospital for Neurology and Neurosurgery and The Institute of Neurology, London.

2.2. Data Aquisition

T2*-weighted echo-planar functional brain volumes were acquired using the Siemens Trio 3T system (Siemens, Erlangen, Germany). For each participant, three sessions were run with 430 volumes each for a total of 1290 volumes per participant. Images were acquired at a volume repetition time (TR) of 2176 milliseconds with an in-plane resolution of 3 × 3 mm, 2 mm slice thickness, and 1 mm slice gap, with echo time = 30 msec and a flip angle of 90°. We discarded the two volumes commencing each session to avoid magnetic equilibrium contamination. (See Furl et al., 2011).

2.3. Experimental Design

The experimental design included a repetition suppression paradigm. Stimuli comprised of images of emotional faces taken from the KDEF database (Lundqvist & Litton, 1998; The Karolinska Directed Emotional Faces, Department of Clinical Neuroscience, Psychology Section, Karolinska Institute) and photographs of cars.

Block designs have been shown to be statistically efficient for DCM and therefore practical for the present study (Mechelli et al., 2013). There were two categories of blocks: faces and cars.

Ninety-six blocks displayed faces and 48 blocks displayed cars, distributed equally over three runs. Each block lasted 15.2 seconds with 4 seconds of fixation between blocks. Eight stimuli with alternating viewpoints (left and right three quarters and frontal) were presented in each block for 1700ms preceded by 200ms fixation. Face blocks varied on whether facial expressions (happy, fearful, neutral, and angry) were different or the same within each block, and whether identities (four male identities) were the same or different within each block. The car blocks varied on whether cars (four cars) were the same or different. All images were grayscaled, normalized to equal luminance mean and range, adjusted to similar size, and placed on a gray background. Faces were cropped to occlude hair and clothing (see Furl et al., 2011).

2.5. Pre-processing and general linear model

Following Furl et al. (2011) data pre-processing was carried out using SPM5 (Wellcome Trust Centre for Neuroimaging, London; http://www.fil.ion.ucl.ac.uk/spm/) with MATLAB (The Mathworks, Natick, MA). Pre-processing comprised realignment, normalization and 8mm spatial smoothing. Slice timing was modeled in the DCM, where the precise acquisition time of each region of interest (ROI) was taken into account. This has been shown to be an effective solution to the slice time problem for DCM (Kiebel et al., 2007).

For ROI definition, we used general linear models (GLMs) from SPM8. First we analyzed the timeseries data at the individual-participant level using a canonical hemodynamic response function, a low-pass filter of 1/256Hz, AR(1) autocorrelation modeling, motion correction, and proportional scaling. Then, contrasts of interest (faces versus cars and all stimuli versus baseline, see ROI selection) were computed in each individual participant. The resulting contrast images were subjected, at a second level, to right-sided t-tests treating participants as random effects. Results images from the second level were thresholded at $P<0.005$ (uncorrected) and clusters were then identified that met family-wise error correction at $P<0.05$ across either the whole brain or a priori small volume correction using Gaussian random field theory.

In order to optimize the SPM for DCM, individual-participant level GLMs were recomputed in SPM12b using regressors for all visual inputs (faces and cars) and faces only (these regressors were collapsed over repetition condition and session), as well as covariates for each run and for head motion. This allows us to assess the effective connectivity of face-selective information across all three runs.

2.6. ROI Selection

We selected ROIs considered "core" face processing areas (i.e. OFA, FFA and pSTS) (Haxby et al., 2000). We also selected ATL, because of its putative role in face recognition and coupling to areas in the core system (Behrmann et al, 2007; Eifuku et al., 2004; Haxby et al., 2000; Yang et al., 2014). Together, these areas were hypothesized to be the main occipito-temporal components in a circuit that processes faces. For inclusion in DCM, these areas had to show significant face selectivity at a second (group) level, right-sided, t-test of 'all faces > all cars' contrast using all participants (both controls and DP). From these criteria, we identified five face-selective ROIs: right OFA (rOFA), right FFA (rFFA), right posterior STS (rpSTS), left FFA (lFFA), and left ATL (lATL). rOFA, lFFA and lATL were small volume corrected using a 10mm sphere around the functional peak coordinates of at least one previous study (Allison, Puce, & McCarthy, 2000; Andrews & Ewbank, 2004; Fox et al., 2009; Hein & Knight, 2008; Rotshtein et al., 2005; Von Der Heide et al., 2013; Winston et al., 2004).

We also selected early visual cortex (EVC) as an ROI for DCM. EVC is not face-selective, but is the first cortical area in the visual processing stream, and, as expected, responded robustly to both faces and cars. Using models that assume that the information initially passes through EVC allows us to estimate the signal sent into the face-selective system in a biologically plausible manner, instead of assuming that the signal remains unchanged until reaching a face-selective area. Such models also allow us to explore pertinent theoretical explanations for face selectivity in which face-selective areas are receptive to low-level face-diagnostic information already present in early visual areas (See Discussion). We identified EVC using a second level one-sample, right-sided, t-

194 test on an '(all faces + all cars) > rest' contrast, and identified the peak activation around the
195 posterior occipital lobes.

196 In accordance with conventional methods, we identified the locations of the ROIs in each
197 individual participant (den Ouden et al., 2012; Grefkes et al., 2008; Mechelli et al., 2003; Mechelli
198 et al., 2004). Using the second-level (group) clusters to define a search space, we identified the
199 individual participants' face-selective peak voxel within the second level clusters (for EVC the
200 visual versus baseline peak voxel was identified). Second level (group) clusters used for search
201 spaces consist of all voxels around the area of interest, which SPM recognized as a single cluster
202 around the peak voxel. The clusters were identified with a significance level at an uncorrected
203 threshold of $p<0.005$ in a second level SPM analysis. If a second level (group) cluster was
204 overlapping with another area, we limited the inclusion of $p<0.005$ thresholded voxels within 10mm
205 of the peak voxel of the area. This was relevant for EVC, rSTS and lATL. In order to ensure that the
206 search spaces were not dominated by one of the groups, we also computed the clusters from each of
207 the groups separately. We found that the peak of the control group and DP group clusters were
208 located within the search spaces, which indicates that our search spaces were representative for each
209 group. After identification of individual peak voxels for all selected ROIs, we created 6mm spheres
210 with no threshold around the peak voxels to create participant-specific ROIs. We extracted ROI
211 mean percentage signal change across voxels (faces>cars contrast for face-selective areas and all
212 visual>rest contrast for EVC) for ROI analysis using MarsBar 0.42 (Brett et al., 2002). This
213 approach reduces the multiple comparison problem from a voxel-wise issue to one involving only
214 the number of ROIs investigated. This is done by focusing only on the activity within the ROI
215 chosen (i.e. six ROIs), and removing the variability between voxel signals within the ROI by
216 averaging the signal of the voxels, and therefore treating each ROI as a single signal measurement
217 (Poldrack, 2007). We used two-sample, two-tailed, t-tests for testing group differences in ROI face
218 selectivity. The analyses were multiple comparison corrected for the number ROIs tested (Poldrack,
219 2007). For DCM, the first eigenvariate timeseries of all participant-specific ROIs were extracted

from the individual participant analyses.

2.7. Dynamic Causal Modeling

DCM uses a generative Bayesian model of effective connectivity between hidden neuronal responses to predict fMRI BOLD responses in pre-specified areas (Friston et al., 2003). DCM allows testing of specific hypotheses regarding effective connectivity. It uses Bayesian model selection (BMS) to determine which model of connectivity best explains the data. Furthermore, it allows for inference on individual connection parameters within a GLM framework (Penny et al., 2004; Stephan et al., 2010). It allows inference on three types of parameters. Endogenous connectivity (A parameters) is the estimated effective connectivity averaged over conditions. Modulatory connectivity (B parameters) models effects of a specific experimental factor on effective connectivity. Last, exogenous parameters (C parameters) model stimulus input effects on areas in the specified system. In the present paper, our primary interest was in measuring connections that are modulated by faces (B parameters). We used DCM12 to carry out the DCM.

2.7.1. Model Selection and Parameter Analysis

Our first goal was to ascertain a model architecture that demonstrates a likely mechanism for producing face selectivity in our face-selective ROIs. Once this model was established, we then could test whether this face selectivity generating mechanism differed in participants with DP and controls. Such differences would provide a potential account of the reductions in face selectivity in posterior areas that we observed in our sample of participants with DP (see also Furl et al., 2011).

We used bayesian model selection (BMS) to infer which model best explained the data (Penny et al., 2004). This approach is based on the posterior probability associated with each model's evidence (Free energy), summed across the participants. We performed BMS on the whole sample and separately for the control and DP groups to estimate the most likely model architecture for every group.

Using Bayesian model averaging (BMA), we estimated A, B, and C parameters, averaged over the model space and weighted by the exceedance probability of each model (the likelihood that

one model is more likely than any other model, given all participant data). This approach to parameter estimation does not assume that participants all use the same model, but allows for different participants to have different model weighting (Penny et al., 2010; Stephan et al., 2010).

We compared the B parameters of controls versus DP participants. This analysis included face modulated connections present in the model architecture showing highest posterior probability in BMS (Fig. 1). This model architecture accounts for the flow of face information in the present data and so differences in face-modulation strength in this model architecture may be relevant for the functional abnormalities in DP. We tested if controls show greater face modulation than participants with DP by submitting B parameters (modulation by faces) to two-sample, right-sided, t-tests. The analyses were multiple comparison (Bonferroni) corrected for number of connections tested.

2.7.2. Specification of Model Space

To identify which connections were most likely to create face selectivity in the face-selective ROIs, we tested modulation by faces on different configurations of connections. Given no a priori assumptions about how non-specific visual information spreads through the system, we endogenously connected all areas reciprocally in all models. We assumed EVC to be the exogenous input area (where activity is driven by all visual experimental stimuli) (see section on ROI selection).

This template was used to formulate the thirteen models that we tested (Fig. 1). The first six models were motivated by the Haxby et al. (2000) model of face processing and, specifically, the features of this model that refer to visual analysis of faces (i.e., a dedicated ”core” system). In models 1-3, face selectivity arises from face modulation between areas in the core system alone (i.e. between rOFA, FFA, and rpSTS), with feedforward (model 1), backward (model 2) or reciprocal (model 3) face modulation. In models 4-6, face selectivity arises from modulation by faces between the core system and lATL with either feedforward (model 4), backward (model 5) or reciprocal (model 6) modulation. In models 7-9, face selectivity arises from interactions between EVC and

downstream face-selective areas. These three models instantiate networks where faces are discriminated from other objects through a feedforward mechanism from EVC. Faces could modulate feedforward connections from EVC to rOFA (model 7), to the core system (model 8) or to all face-selective areas (model 9). In models 10 and 11, face selectivity arises from backward/feedback modulation by faces from ATL to FFA (model 10), or to the core system (model 11). Finally, in models 12 and 13, face selectivity arises through horizontal modulation by faces between left and right FFA (model 12), or between FFA and STS (model 13). This model space explores the network mechanisms that are currently plausible for the selected areas, including possible feedforward, backward and reciprocal interactions between EVC, core system and anterior temporal areas.

3. Results

3.1. SPM Group Analysis and ROI analysis

We performed an SPM group analysis of all the participants to test for face selectivity (i.e. faces>cars contrast) and to identify face-selective ROIs for DCM. Significant clusters and peaks at $P<0.05$ (family-wise error corrected) were identified. We observed significant face selectivity in rOFA, bilateral FFA, rpSTS, bilateral amygdala, precuneus, orbito-frontal cortex, and lATL. From these results and from our *a priori* assumption that occipito-temporal face-selective areas are associated with face recognition, we selected for DCM the face-selective areas rOFA, bilateral FFA, rpSTS and lATL (Fig. 2). Furl et al. (2011) already reported the face selectivity results separately for controls and DPs and found similar results. Here, the analysis combined all participants, as we intended to use the second level (group) results to define a search space for ROI definition that could be applied to the whole sample.

We also report an ROI analysis using the participant-specific ROIs that we obtained from the whole sample search space and that we included in the DCM (Fig. 3). All p-values for this ROI analysis are reported as uncorrected and are inferred to be significant according to a Bonferroni

298 corrected alpha value: α = 0.0083 (α = 0.05/6). We observed significantly greater face selectivity in
299 controls compared to the DP group in rFFA $t(28) = 3.304$, $p = 0.0026$, lFFA $t(28) = 3.172$, $p =$
300 0.0037 and rpSTS $t(28) = 2.970$, $p = 0.0061$. We found no significant group difference in face
301 selectivity following Bonferroni correction in rOFA $t(28) = 0.379$, $p = 0.708$ and lATL $t(28)=2.691$,
302 $p = 0.012$, as well as no significant group difference in BOLD response (all visual>rest) in EVC
303 $t(28) = 1{,}994$, $p = 0.055$. These results generally agree with the results found in Furl et al. (2011).
304 However, we also identified an additional role for rSTS in DP and the comparion of lATL face-
305 selectivity in controls and DPs narrowly failed to reach significance after Bonferroni correction.
306
307 ## *3.2. Dynamic Causal Modeling*
308 ### 3.2.1. Bayesian Model Selection
309 The model in which faces modulate the connections from EVC to the core system (EVC to
310 Core (Model 8)) achieved a posterior probability of approximately 1.0 in both groups and in the
311 whole sample (Table 1; Fig. 1). Model architecture in DP and control groups was therefore
312 qualitatively similar.
313 Face processing is often regarded as primarily lateralized to the right hemisphere. To test if
314 some models were less likely due to inter-hemispheric connections (e.g. rOFA to lFFA), we also ran
315 a post-hoc model space only containing areas from the right hemisphere as well as EVC (EVC,
316 rOFA, rFFA, rSTS). Again these results showed that EVC to core areas was the most probable
317 model in a BMS including all participants (posterior probability for EVC to core ~ 1). This makes
318 us confident that the original model space was not biased by inter-hemispheric connections in the
319 model space, and all subsequent analysis are based on the original model space.
320
321 ### 3.2.2. Face Modulation Parameters
322 We assessed the difference between controls and DPs in the magnitudes of their face-
323 modulated B connections, which we considered relevant for face processing. We selected for

comparison the four face-modulated connections present in the model architecture that had the highest posterior probability in both groups (i.e. Model 8). All p-values are reported as uncorrected and are inferred to be significant according to a Bonferroni corrected alpha value $\alpha = 0.0125$ ($\alpha = 0.05/4$).

Three out of the four effective connections that were modulated by faces in the most likely model architecture showed altered modulation strength between control and DP (Fig. 4). Face modulation on the connection from EVC to rOFA did not show a significantly greater face modulation for controls compared to the DP group $t(28) = -0.110$, $p = 0.5432$. In contrast, we found significantly greater face modulation for controls compared to the DP group on the connections from EVC to rFFA $t(28) = 2.536$, $p = 0.0085$, from EVC to lFFA $t(28) = 2.253$, $p = 0.0088$ and from EVC to rpSTS $t(28) = 2.912$, $p = 0.0035$.

4. Discussion

We aimed to understand network properties contributing to face processing and how these network properties support accurate face recognition. We assessed this latter question by investigating how the face processing network is altered in DP individuals, who cannot accurately recognize faces. We focused on effective connectivity using DCM and show that the network model that best explains how face-relevant information flows through a face-selective network is one where the presence or absence of faces modulates feedforward effective connectivity from EVC to occipito-temporal areas (OFA, FFA and STS). This model was selected out of 13 different models in a BMS and best explained our data when analyzing DP and control groups separately or combined. We then related the properties of this network to facial recognition ability by testing for differences in modulation strength between DP and control groups on model-relevant parameters (i.e. modulation parameters present in the model which best explained our data). We found that modulation of connections from EVC to rFFA, lFFA, and rpSTS was significantly diminished in DP, relative to controls. Our results indicate that these connections may contribute to normal face-

selective responses as well as accurate facial recognition.

4.1. Connections that give rise to face-selective responses

Most previous studies investigating directional flow of information between face-selective areas have not contrasted face information versus other types of object stimuli when testing for modulations of effective connectivity (Fairhall and Ishai, 2007; Ewbank et al., 2013). The advantage of quantifying the relative contribution of face-specific modulation to connectivity strength is that it allows for an inference of how face selectivity arises as a function of connectivity. The few studies that modeled the effect of faces compared to other stimuli considered model spaces with relatively few regions (Furl et al., 2014; Nagy et al., 2012). Here, we have performed the most comprehensive model space to date and found that the model that best explained our data contained face-modulated connections from EVC to occipito-temporal areas.

We found that models (inspired by Haxby et al. (2000)) where connections from OFA to FFA and STS created face selectivity in occipito-temporal areas were suboptimal. This result is consistent with findings in patients with lesions covering face-selective areas. Steeves et al. (2006) presented a patient (DF) who had bilateral lesion of OFA, but continued to show face selectivity in FFA and STS. Similarly, patient PS who had lesioned rOFA and lFFA showed preserved face-selective responses in rFFA (Rossion et al., 2003). In addition, two patients with lesioned rOFA and rFFA still had face selective responses in rpSTS (Dalrymple et al., 2011). These neuropsychological studies are in accordance with a model where face selectivity is created through effective connectivity from EVC to all core face processing areas (OFA, FFA, and STS).

Several of the models that we tested were theoretically motivated, but were nevertheless found to be sub-optimal. For example, our results offer support for some features of the model proposed by Haxby et al. (2000). Our results agree on "core" areas responsible for visual analysis (OFA, FFA, pSTS). We found that face selectivity in the core areas was driven by visual cortex. Nevertheless, Haxby et al. (2000) further predicts that FFA and STS receive facial feature

information from OFA. We did not find a special role for OFA in driving face selectivity in FFA and STS. Our results instead partly accord with a previous study showing face-relevant effective connectivity from Brodmann area 18 (BA18) (partly equivalent to EVC here). Furl et al. (2014) showed that face modulation on the connection from BA18 to OFA (but not FFA) partly creates face selectivity in posterior occipito-temporal areas.

Our model space also tested the possibility that backward influences, including those from ATL, contributed to face selectivity. The present results suggest no role for ATL in creating face-selective responses in posterior areas. Instead, the face-selective responses observed in ATL appear to be either a function of the dynamics created in the interaction between EVC and occipito-temporal areas or a result of a mechanism that was not captured in the present model space. For example, face selectivity generated in core areas (resulting from their coupling with EVC) could be propagated forward to ATL via endogenous (unmodulated) connections. It should be noted that these results do not imply that interactions between other areas do not occur or are not involved in generating other functional responses that are relevant to face processing. We show that face-selective occipito-temporal responses are supported by effective connectivity from EVC to occipito-temporal core areas, rather than by interactions between different core areas or ATL.

4.2. A network-based account of diminished face recognition ability in DP

DP has been proposed to result from a disconnection between posterior and anterior face-selective areas (Behrmann & Plaut, 2013), in part, on the basis of diffusion tensor imaging (DTI) results. Thomas et al. (2008) found evidence for diminished axonal integrity in major pathways projecting between posterior occipito-temporal areas and anterior areas in ATL and frontal cortex. Because Avidan et al. (2005) found evidence that functional BOLD signal is not altered in DP within occipito-temporal areas, Thomas et al. (2008) proposed that DP is related to disconnection with ATL, rather than dysfunctional processing in posterior occipito-temporal areas. However, more recently, two studies reported that white matter deficits were not present in major pathways in DP;

instead DP was associated with atypical white matter structure around the FFA (Gomez et al., 2014; Song et al., 2015). These findings are in accordance with our findings implicating the connectivity of FFA in face processing. A limitation of previous studies investigating DP is the small sample sizes such as four (Avidan et al., 2005) or six (Thomas et al., 2008) participants with DP and the lack of appropriately-powered group statistics. In contrast, our data (15 DP and 15 control participants) showed that DP had diminished BOLD response in posterior occipito-temporal areas (originally reported in Furl et al., 2011; and see Dinckelacker et al. (2011) and von Kriegstein et al. (2008)). We here expand on the results by Furl et al. (2011) by identifying potential network explanations for the differences between DP and the normal population. In this study we find evidence for diminished effective connectivity from EVC to FFA, and EVC to pSTS that results in reduced activation in occipito-temporal areas to faces, compared to other objects, as well as reduced face recognition performance (Furl et al., 2011).

Avidan et al. (2014) found reduced functional connectivity between core areas and ATL. However, in the present study, the model identified to be most likely to give rise to face selectivity (model 8) did not contain face-modulated effective connectivity to or from lATL. lATL connections, therefore, are not a good candidate for explaining the reduced face selectivity observed in posterior areas in our sample of DP participants. Nevertheless, there is reduced grey matter and functional responses in ATL associated with DP (Behrmann et al., 2007; Garrido et al., 2009; Furl et al., 2011). It is possible that these abnormalities in the ATL of people with DP may instead be caused by chronically diminished propagation of face-specific activity from more posterior areas, or they may be a separate manifestation of the dysfunctions associated with DP.

4.3. Conclusions

We have presented evidence for a model of how face selectivity arises in the human brain and how this model is compromised in DP. We have shown that a model in which face selectivity arises from effective connectivity from EVC to posterior occipito-temporal areas is more likely than

other plausible models tested. Furthermore, we suggest that the functional BOLD response in FFA and rpSTS and behavioral deficits in DP can partly be accounted for by diminished effective connectivity from EVC to posterior occipito-temporal areas.

References

Allison, T., Puce, A., & McCarthy, G. (2000). Social perception from visual cues: Role of the STS region. *Trends in Cognitive Sciences*, *4*(7), 267–278. http://doi.org/10.1016/S1364-6613(00)01501-1

Andrews, T. J., & Ewbank, M. P. (2004). Distinct representations for facial identity and changeable aspects of faces in the human temporal lobe. *NeuroImage*, *23*(3), 905–913. http://doi.org/10.1016/j.neuroimage.2004.07.060

Avidan, G., Hasson, U., Malach, R., & Behrmann, M. (2005). Detailed exploration of face-related processing in congenital prosopagnosia: 2. Functional neuroimaging findings. *Journal of Cognitive Neuroscience*, *17*(7), 1150–1167. http://doi.org/10.1162/0898929054475154

Avidan, G., Tanzer, M., Hadj-Bouziane, F., Liu, N., Ungerleider, L. G., & Behrmann, M. (2014). Selective dissociation between core and extended regions of the face processing network in congenital prosopagnosia. *Cerebral Cortex*, *24*(6), 1565–1578. http://doi.org/10.1093/cercor/bht007

Behrmann & Avidan. (2005). Congenital prosopagnosia: face-\nblind from birth . *Trends in Cognitive Neuroscience, 9*(4), 180-187. doi:10.1016/j.tics.2005.02.011

Behrmann, M., Avidan, G., Gao, F., & Black, S. (2007). Structural imaging reveals anatomical alterations in inferotemporal cortex in congenital prosopagnosia. *Cerebral Cortex*, *17*(10), 2354–2363. http://doi.org/10.1093/cercor/bhl144

Behrmann, M., & Plaut, D. C. (2013). Distributed circuits, not circumscribed centers, mediate visual recognition. *Trends in Cognitive Sciences*, *17*(5), 210–219.

http://doi.org/10.1016/j.tics.2013.03.007

Brett, M, Anton, J, Valabregue, R, Poline, J. (2002). Region of interest analysis using an SPM toolbox [abstract] *Presented at the 8th International Conference on Functional Mapping of the Human Brain*, June 2-6,, Sendai, Japan. Available on CD-ROM in NeuroImage, Vol 16, No 2

Dalrymple, K. a., Oruç, I., Duchaine, B., Pancaroglu, R., Fox, C. J., Iaria, G., Barton, J. J. S. (2011). The anatomic basis of the right face-selective N170 IN acquired prosopagnosia: A combined ERP/fMRI study. *Neuropsychologia*, *49*(9), 2553–2563. http://doi.org/10.1016/j.neuropsychologia.2011.05.003

Den Ouden, D. B., Saur, D., Mader, W., Schelter, B., Lukic, S., Wali, E., Thompson, C. K. (2012). Network modulation during complex syntactic processing. *NeuroImage*, *59*(1), 815–823. http://doi.org/10.1016/j.neuroimage.2011.07.057

Dinckelacker, V., Gruter, M., Klaver, P., Gruter, T., Specht, K., Weis, S., Kennerknecht, I., Elger, C.E., Fernandez., G. (2011). Congenital prosopagnosia: multistage anatomical and functional deficits in face processing circuitry. *Journal of Neurology, 258,* 770-782. http://doi.org/10.1007/s00415-010-5828-5

Duchaine, B., & Nakayama, K. (2005). Dissociations of face and object recognition in developmental prosopagnosia. *Journal of Cognitive Neuroscience*, *17*(2), 249–261. http://doi.org/10.1162/0898929053124857

Duchaine, B., & Nakayama, K. (2006). The Cambridge Face Memory Test: Results for neurologically intact individuals and an investigation of its validity using inverted face stimuli and prosopagnosic participants. *Neuropsychologia*, *44*(4), 576–585. http://doi.org/10.1016/j.neuropsychologia.2005.07.001

Eifuku, S., De Souza, W. C., Tamura, R., Nishijo, H., & Ono, T. (2004). Neuronal correlates of face identification in the monkey anterior temporal cortical areas. *Journal of Neurophysiology*, *91*(1), 358–371. http://doi.org/10.1152/jn.00198.2003

478 Ewbank, M. P., Henson, R. N., Rowe, J. B., Stoyanova, R. S., & Calder, A. J. (2013). Different
479 neural mechanisms within occipitotemporal cortex underlie repetition suppression across same
480 and different-size faces. *Cerebral Cortex*, *23*(5), 1073–1084.
481 http://doi.org/10.1093/cercor/bhs070

482 Fairhall, S. L., & Ishai, A. (2007). Effective connectivity within the distributed cortical network for
483 face perception. *Cerebral Cortex*, *17*(10), 2400–2406. http://doi.org/10.1093/cercor/bhl148

484 Fox, C. J., Moon, S. Y., Iaria, G., & Barton, J. J. S. (2009). The correlates of subjective perception
485 of identity and expression in the face network: An fMRI adaptation study. *NeuroImage*, *44*(2),
486 569–580. http://doi.org/10.1016/j.neuroimage.2008.09.011

487 Friston, K. J., Harrison, L., & Penny, W. (2003). Dynamic causal modeling. *Neuroimage*, *19*(4),
488 1273–1302. http://doi.org/10.1016/S1053-8119(03)00202-7

489 Furl, N., Coppola, R., Averbeck, B. B., & Weinberger, D. R. (2013). Cross-Frequency Power
490 Coupling Between Hierarchically Organized Face-Selective Areas. *Cerebral Cortex*, 2409–
491 2420. http://doi.org/10.1093/cercor/bht097

492 Furl, N., Garrido, L., Dolan, R. J., Driver, J., & Duchaine, B. (2011). Fusiform gyrus face selectivity
493 relates to individual differences in facial recognition ability. *Journal of Cognitive*
494 *Neuroscience*, *23*(7), 1723–1740. http://doi.org/10.1162/jocn.2010.21545

495 Furl, N., Henson, R. N., Friston, K. J., & Calder, A. J. (2014). Network Interactions Explain
496 Sensitivity to Dynamic Faces in the Superior Temporal Sulcus. *Cerebral Cortex*, *1*, 1–7.
497 http://doi.org/10.1093/cercor/bhu083

498 Garrido, L., Furl, N., Draganski, B., Weiskopf, N., Stevens, J., Tan, G. C. Y., Duchaine, B. (2009).
499 Voxel-based morphometry reveals reduced grey matter volume in the temporal cortex of
500 developmental prosopagnosics. *Brain*, *132*(12), 3443–3455.
501 http://doi.org/10.1093/brain/awp271

502 George, N., Driver, J., & Dolan, R. J. (2001). Seen gaze-direction modulates fusiform activity and

its coupling with other brain areas during face processing. *NeuroImage*, *13*(6), 1102–1112. http://doi.org/10.1006/nimg.2001.0769

Gomez J, Pestilli F, Yoon J, Grill-Spector K. (2015). Functionally defined white matter reveals segregated pathways in human ventral temporal cortex associated with category-specific processing. *Neuron* 85: 216-227

Grefkes, C., Eickhoff, S. B., Nowak, D. a., Dafotakis, M., & Fink, G. R. (2008). Dynamic intra- and interhemispheric interactions during unilateral and bilateral hand movements assessed with fMRI and DCM. *NeuroImage*, *41*(4), 1382–1394. http://doi.org/10.1016/j.neuroimage.2008.03.048

Gschwind, M., Pourtois, G., Schwartz, S., Van De Ville, D., & Vuilleumier, P. (2012). White-matter connectivity between face-responsive regions in the human brain. *Cerebral Cortex*, *22*(7), 1564–1576. http://doi.org/10.1093/cercor/bhr226

Haxby, J. V, Hoffman, E. A., & Gobbini, M. I. (2000). The distributed human neural system for face perception, *Trends in Cognitive Neuroscience, 4*(6), 223–233. http://doi.org/10.1016/S1364-6613(00)01482-0

Hein, G., & Knight, R. T. (2008). Superior temporal sulcus--It's my area: or is it? *Journal of Cognitive Neuroscience*, *20*(12), 2125–2136. http://doi.org/10.1162/jocn.2008.20148

Iidaka, T., Omori, M., Murata, T., Kosaka, H., Yonekura, Y., Okada, T., & Sadato, N. (2001). Neural interaction of the amygdala with the prefrontal and temporal cortices in the processing of facial expressions as revealed by fMRI. *Journal of Cognitive Neuroscience*, *13*(8), 1035–1047. http://doi.org/10.1162/089892901753294338

Kanwisher, N., McDermott, J., & Chun, M. M. (1997). The fusiform face area: a module in human extrastriate cortex specialized for face perception. *The Journal of Neuroscience : The Official Journal of the Society for Neuroscience*, *17*(11), 4302–4311. http://doi.org/10.1098/Rstb.2006.1934

528 Kiebel, S. J., Klöppel, S., Weiskopf, N., & Friston, K. J. (2007). Dynamic causal modeling: A
529 generative model of slice timing in fMRI. *NeuroImage*, *34*(4), 1487–1496.
530 http://doi.org/10.1016/j.neuroimage.2006.10.026

531 Mechelli, A., Price, C. J., Friston, K. J., & Ishai, A. (2004). Where bottom-up meets top-down:
532 Neuronal interactions during perception and imagery. *Cerebral Cortex*, *14*(11), 1256–1265.
533 http://doi.org/10.1093/cercor/bhh087

534 Mechelli, A., Price, C. J., Henson, R. N. a, & Friston, K. J. (2003). Estimating efficiency a priori: A
535 comparison of blocked and randomized designs. *NeuroImage*, *18*(3), 798–805.
536 http://doi.org/10.1016/S1053-8119(02)00040-X

537 Mechelli, A., Price, C. J., Noppeney, U., & Friston, K. J. (2003). A dynamic causal modeling study
538 on category effects: bottom-up or top-down mediation? *Journal of Cognitive Neuroscience*,
539 *15*(7), 925–934. http://doi.org/10.1162/089892903770007317

540 Moeller, S., Freiwald, W. a, & Tsao, D. Y. (2008). Patches with links: a unified system for
541 processing faces in the macaque temporal lobe. *Science*, *320*(5881), 1355–1359.
542 http://doi.org/10.1126/science.1157436

543 Nunn, J. a, Postma, P., & Pearson, R. (2001). Developmental prosopagnosia: should it be taken at
544 face value? *Neurocase : Case Studies in Neuropsychology, Neuropsychiatry, and Behavioural*
545 *Neurology*, *7*(1), 15–27. http://doi.org/10.1093/neucas/7.1.15

546 Penny, W. D., Stephan, K. E., Daunizeau, J., Rosa, M. J., Friston, K. J., Schofield, T. M., & Leff, A.
547 P. (2010). Comparing families of dynamic causal models. *PLoS Computational Biology*, *6*(3).
548 http://doi.org/10.1371/journal.pcbi.1000709

549 Penny, W. D., Stephan, K. E., Mechelli, a, & Friston, K. J. (2004). Comparing dynamic causal
550 models. *Ni*, *22*(3), 1157–1172.

551 Poldrack R.A (2007). Region of interest analysis for fMRI. *Social Cognitive and Affective*
552 *Neuroscience. 2*(1). 67-70. doi: 10.1093/scan/nsm006

553 Rossion, B., Caldara, R., Seghier, M., Schuller, A. M., Lazeyras, F., & Mayer, E. (2003). A network
554 of occipito-temporal face-sensitive areas besides the right middle fusiform gyrus is necessary
555 for normal face processing. *Brain*, *126*(11), 2381–2395. http://doi.org/10.1093/brain/awg241

556 Rotshtein, P., Henson, R. N. a, Treves, A., Driver, J., & Dolan, R. J. (2005). Morphing Marilyn into
557 Maggie dissociates physical and identity face representations in the brain. *Nature*
558 *Neuroscience*, *8*(1), 107–113. http://doi.org/10.1038/nn1370

559 Song, S., Garrido, L., Nagy, Z., Mahammadi, S., Steel, A., Driver, J., Dolan, R.J., Duchaine, B.,
560 Furl, N. (2015). Local but not long-range microstructural differences of the ventral temporal
561 cortex in developmental prosopagnosia. *Neuropsychologia*. 78. 195-206
562 **doi:10.1016/j.neuropsychologia.2015.10.010**

563 Steeves, J. K., Culham, J. C., Duchaine, B. C., Pratesi, C. C., Valyear, K. F., Schindler, I.,
564 Humphrey, G. K., Milner, A. D., Goodale, M. A. (2006). The fusiform face area is not
565 sufficient for face recognition: Evidence from a patient with dense prosopagnosia and no
566 occipital face area. *Neuropsychologia*, *44*(4), 594–609.
567 http://doi.org/10.1016/j.neuropsychologia.2005.06.013

568 Stephan, K. E., Penny, W. D., Moran, R. J., den Ouden, H. E. M., Daunizeau, J., & Friston, K. J.
569 (2010). Ten simple rules for dynamic causal modeling. *NeuroImage*, *49*(4), 3099–3109.
570 http://doi.org/10.1016/j.neuroimage.2009.11.015

571 Thomas, C., Avidan, G., Humphreys, K., Jung, K., Gao, F., & Behrmann, M. (2009). Reduced
572 structural connectivity in ventral visual cortex in congenital prosopagnosia. *Nature*
573 *Neuroscience*, *12*(1), 29–31. http://doi.org/10.1167/6.6.88

574 Von Der Heide, R. J., Skipper, L. M., & Olson, I. R. (2013). Anterior temporal face patches: a meta-
575 analysis and empirical study. *Frontiers in Human Neuroscience*, *7*(February), 17.
576 http://doi.org/10.3389/fnhum.2013.00017

577 Von Kriegstein, K., Dogan, Ö., Grüter, M., Giraud., A., Kell, C.A., Grüter, T., Kleinschmidt, A.,

Kiebel, S.J., (2008). Simulation of talking faces in the human brain improves auditory speech recognition. *Proceedings of the National Academy of Sciences of the United States of America, 105*(18), 6747-6752

Winston, J. S., Henson, R. N. a, Fine-Goulden, M. R., & Dolan, R. J. (2004). fMRI-adaptation reveals dissociable neural representations of identity and expression in face perception. *Journal of Neurophysiology*, *92*(3), 1830–1839. http://doi.org/10.1152/jn.00155.2004

Yang, H., Susilo, T., & Duchaine, B. (2014). The anterior temporal face area contains invariant representations of identity that can persist despite the loss of right FFA and OFA. *Cerebral Cortex.*

Figure 1: Model space.

Thirteen models were chosen to test different hypotheses about the model architecture giving rise to face selectivity in a occipito-temporal network. The models vary only in which configuration of connections are modulated by faces. The titles above the models summarize which connections are modulated by faces. The colors of the bold lines between areas signify which direction are modulated by faces. All models are fully endogenously connected (including self connections) and have all visual stimuli (Faces and Cars) as driving input to EVC. Model 8 is highlighted, because the BMS showed this model as the best explanation for the data in both groups. Abbreviations: EVC:Early visual cortex, rOFA: Right occipital face area, rFFA: Right fusiform face area, lFFA: Left fusiform area, rpSTS: Right posterior superior temporal sulcus, lATL: Left anterior temporal lobe

Figure 2: SPM group analysis.

SPM group analysis of faces>cars contrast (A,B,C) and faces+cars>baseline (D). Threshold at P<0.005 (uncorrected).

Figure 3: Group differences in ROI signal (faces>cars) intensities for face-selective areas.

Abbreviations: EVC:Early visual cortex, rOFA: Right occipital face area, rFFA: Right fusiform face area, lFFA: Left fusiform area, rpSTS: Right posterior superior temporal sulcus, lATL: Left anterior temporal lobe, * = p<0.05, ** = p< 0.01. Error bars = 1 sem

Figure 4: Group differences in modulation of connectivity by faces.

Abbreviations: EVC: Early visual cortex, rOFA: Right occipital face area, rFFA: Right fusiform face area, lFFA: Left fusiform area, * = p<0.05, ** = p< 0.01. Error bars = 1 sem

Table 1: Bayesian Model Selection

Posterior probabilities for specified model architectures. Posterior probabilities were estimated for control participants and DP participants separately, as well as all participants combined. Model architectures are illustrated in figure 1.

Model Architecture	**Posterior Probability**		
	Controls	DP	All
Backward Core (Model 1)	0	0	0
Forward Core (Model 2)	0	0	0
Reciprocal Core (Model 3)	0	0	0
Backward Core + lATL (Model 4)	0	0	0
Forward Core + lATL (Model 5)	0	0	0
Reciprocal Core + lATL (Model 6)	0	0	0
EVC to rOFA (Model 7)	0	0	0
EVC to Core (Model 8)	1	1	1
EVC to Core + lATL (Model 9)	0	0	0
lATL to Core (Model 10)	0	0	0
lATL to FFA (Model 11)	0	0	0
Reciprocal FFA and rpSTS (Model 12)	0	0	0
Reciprocal FFA (Model 13)	0	0	0

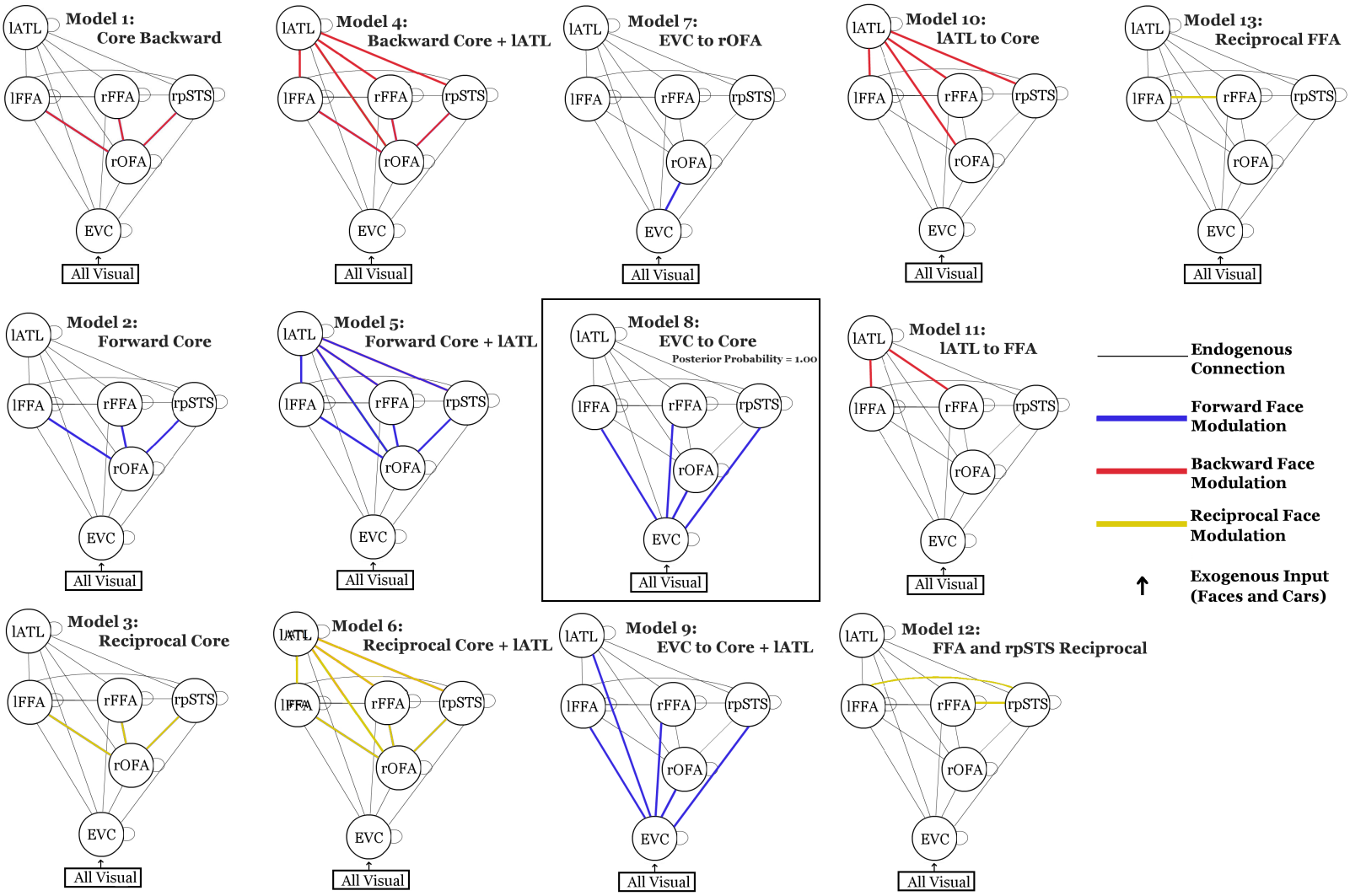
Model 1:
Core Backward
lATL
lFFA
rFFA
rpSTS
rOFA
EVC
All Visual
Model 4:
Backward Core + lATL
Model 7:
EVC to rOFA
Model 10:
lATL to Core
Model 13:
Reciprocal FFA
Model 2:
Forward Core
Model 5:
Forward Core + lATL
Model 8:
EVC to Core
Posterior Probability = 1.00
Model 11:
lATL to FFA
Endogenous Connection
Forward Face Modulation
Backward Face Modulation
Reciprocal Face Modulation
Exogenous Input (Faces and Cars)
Model 3:
Reciprocal Core
Model 6:
Reciprocal Core + lATL
Model 9:
EVC to Core + lATL
Model 12:
FFA and rpSTS Reciprocal

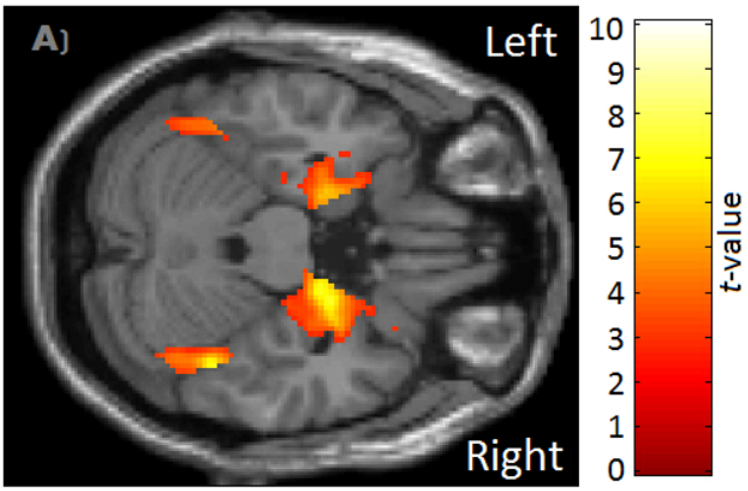

Z = -24, Bilateral FFA (Faces>Cars)

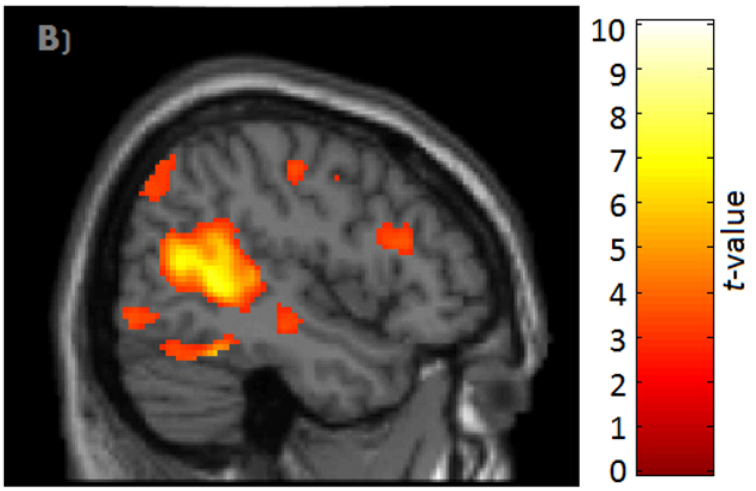

X = 48, rFFA and rpSTS (Faces>Cars)

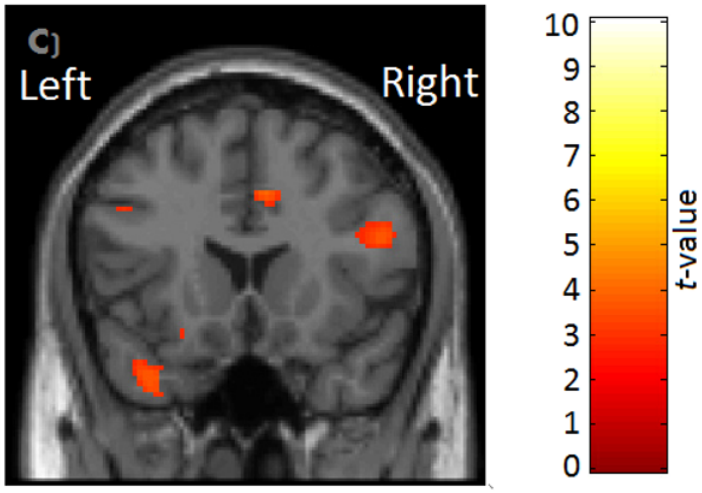

Y = = 18, lATL (Faces>Cars)

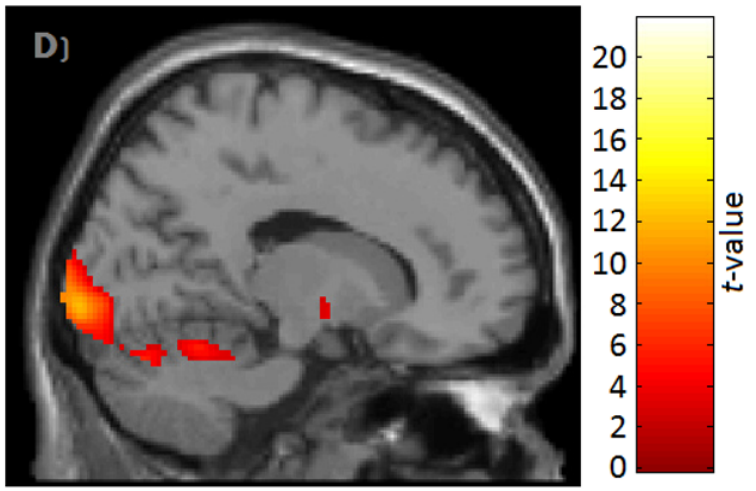

X = 16, EVC (All Visual>Rest)

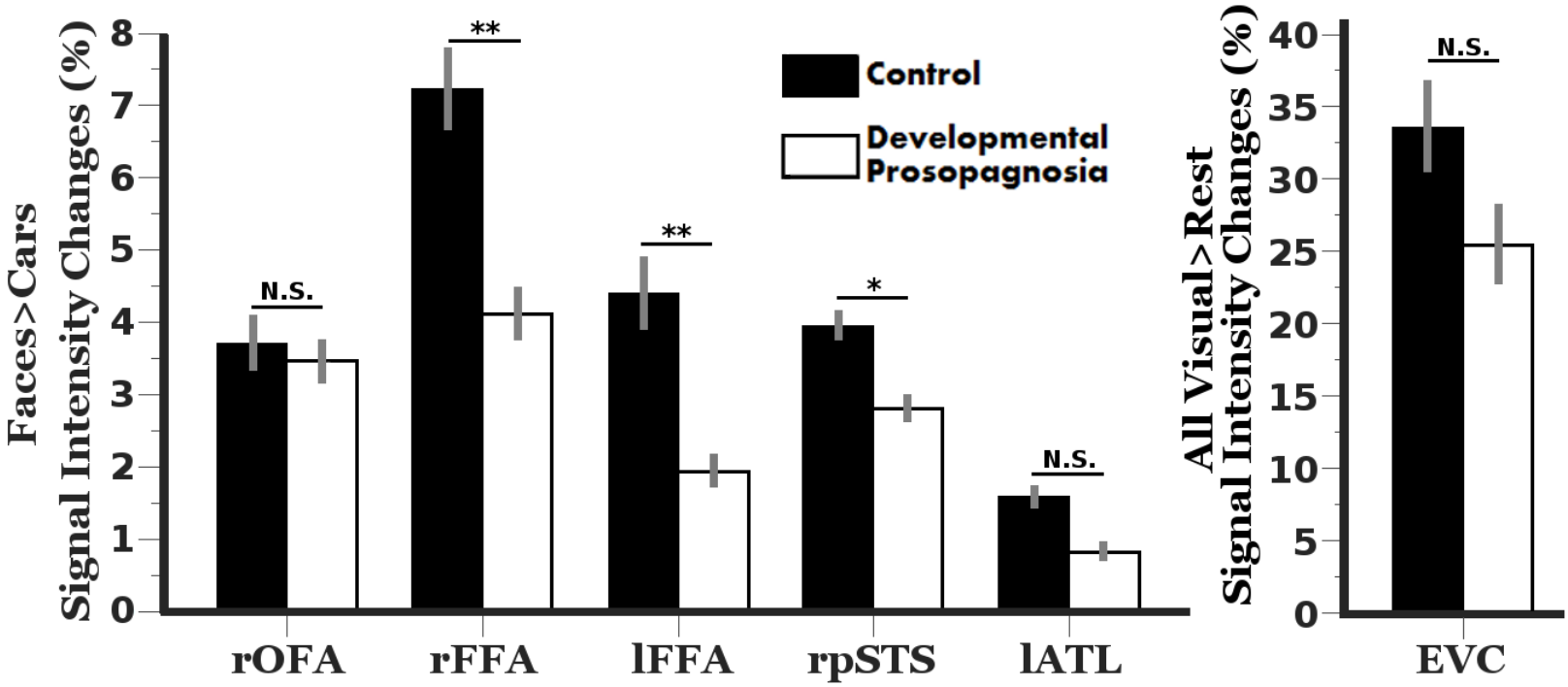
Faces>Cars
Signal Intensity Changes (%)
0
1
2
3
4
5
6
7
8
N.S.
**
**
*
N.S.
Control
Developmental Prosopagnosia
rOFA
rFFA
lFFA
rpSTS
lATL
All Visual>Rest
Signal Intensity Changes (%)
0
5
10
15
20
25
30
35
40
N.S.
EVC

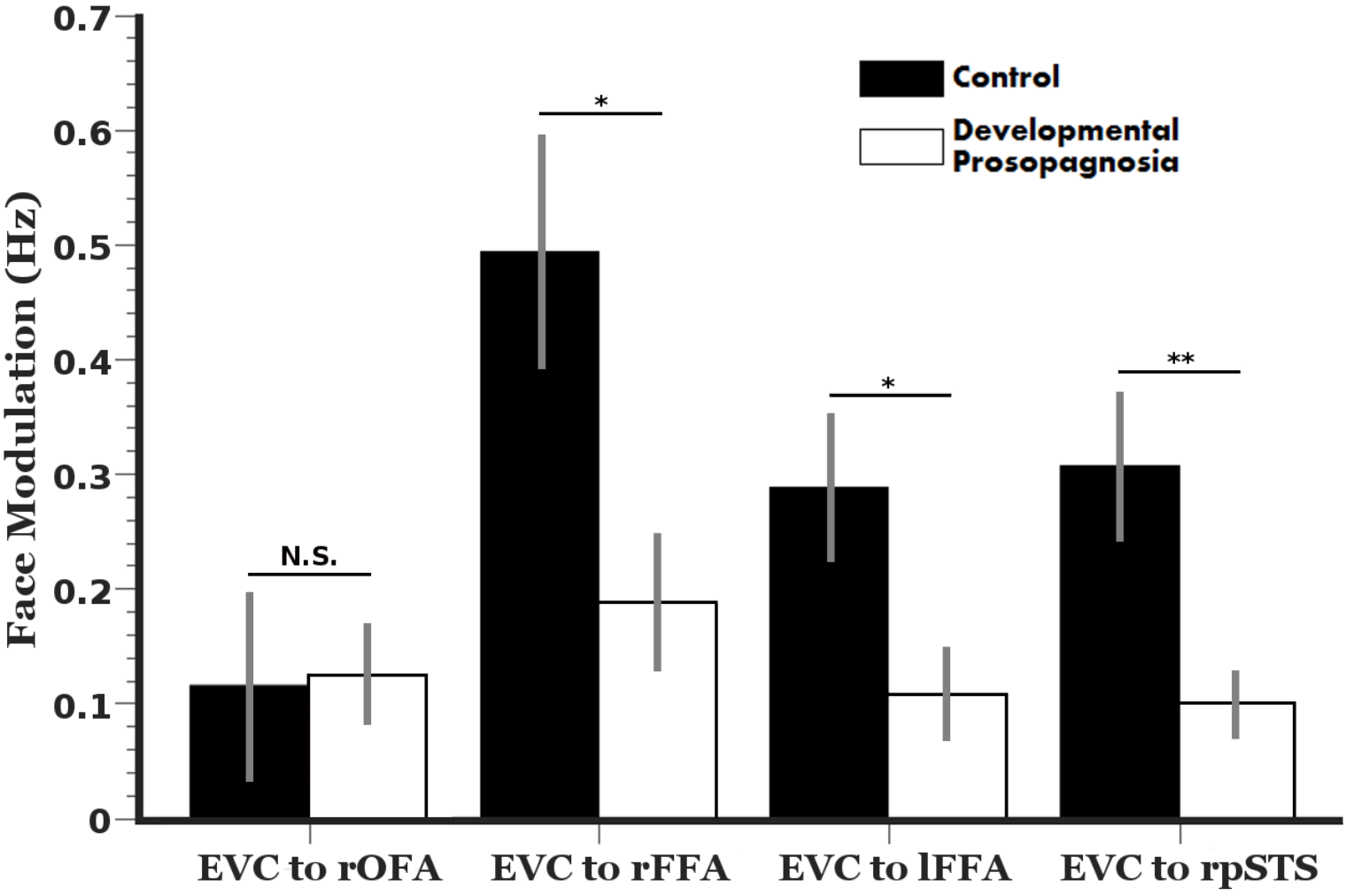
0.7
0.6
0.5
0.4
0.3
0.2
0.1
0
Face Modulation (Hz)
Control
Developmental Prosopagnosia
N.S.
*
*
**
EVC to rOFA
EVC to rFFA
EVC to lFFA
EVC to rpSTS